Deployment of a Class 2 Tensegrity Boom

Jean-Paul Pinaud[a], Soren Solari[a], and Robert E. Skelton[a]

[a]University of California, San Diego
9500 Gilman Drive, La Jolla, California 92093, U.S.A.

Abstract

Tensegrity structures are special truss structures composed of bars in compression and cables in tension. Most tensegrity structures under investigation, to date, have been of *Class 1*, where bars do not touch. In this article, however, we demonstrate the hardware implementation of a 2 stage symmetric *Class 2* tensegrity structure, where bars do connect to each other at a pivot. The open loop control law for tendon lengths to accomplish the desired geometric reconfiguration are computed analytically. The velocity of the structure's height is chosen and reconfiguration is accomplished in a quasi-static manner, ignoring dynamic effects. The main goal of this research was to design, build, and test the capabilities of the Class 2 structure for deployment concepts and to further explore the possibilities of multiple stage structures using the same design and components.

Keywords: Tensegrity structures, deployment, reconfiguration, stable unit

1. INTRODUCTION

Tensegrity structures are built of bars and tendons attached to the ends of the bars.[1] The bars can resist compressive force and the strings cannot. Most bar-string configurations which one might conceive are not in equilibrium, and if actually constructed will collapse to a different shape. Only bar-string configurations in a stable equilibrium will be called tensegrity structures.[2–5]

If well designed, the application of forces to a tensegrity structure will deform it into a slightly different shape in a way which supports the applied forces. Tensegrity structures are very special cases of trusses, where members are assigned special functions. Some members are always in tension and others are always in compression. We will adopt the words "tendons" for the tensile members, and "bars" for compressive members.[6] A tensegrity structure's bars cannot be attached to each other through joints that impart torques. The end of a bar can be attached to tendons or ball jointed to other bars.

Tensegrity structures are natural candidates to be actively controlled structures since the control system can be embedded in the structure directly; for example tendons can act as actuators and/or sensors.[7–9] Shape control of the tensegrity structure can be accomplished by moving along its equilibrium manifold. The tensegrity unit shown in Fig. 1 is the simplest three–dimensional tensegrity unit which comprises three bars held together in space by strings so as to form a tensegrity unit. A tensegrity unit comprising of three bars will be called a 3–bar tensegrity. A 3–bar tensegrity is constructed by using three bars in each stage which are twisted either in clockwise or in anti–clockwise direction. The top strings connecting the top of each bar support the next stage in which the bars are twisted in a direction opposite to the bars in the previous stage. In this way any number of stages can be constructed which will have an alternating clockwise and anti–clockwise rotation of the bars in each successive stage. This is the type of structure in Snelson's Needle Tower.

Contact info:
For animations/movies of figures contact authors.
J.P.Pinaud: Email: jpinaud@mae.ucsd.edu
S. Solari: Email: ssolari@ucsd.edu

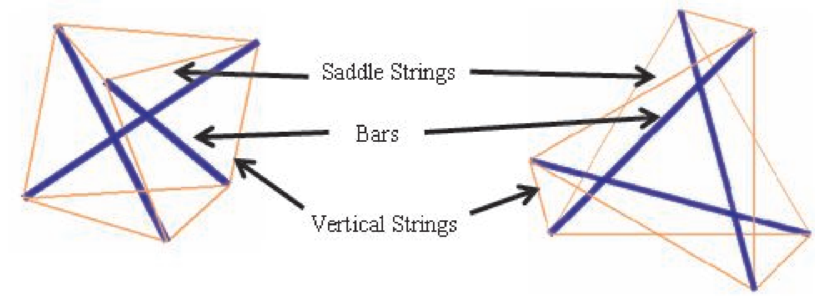

Figure 1. Simplest tensegrity unit: three-bar unit.

In contrast to the Class 1 structure,[10, 11] a Class 2 structure can also be constructed with the same 3–bar tensegrity unit. Assembly of two units, with clockwise and anti–clockwise sense, can be "stacked" directly on each other, resulting in bars connecting shown in Fig. 2a. The following section addresses the analysis and construction of a prototype Class 2 tensegrity structure that verifies the deployment methodology used.

2. TWO STAGE CLASS 2 TENSEGRITY STRUCTURE

Design of a two-stage Class 2 tensegrity structure begins with the design of the base. The allowable twist angle, α, of a two-stage Class 2 structure with fixed base nodes is $\frac{\pi}{2} - \frac{\pi}{n}$, where n is the number of bars in each stage ($n = 3$ in this paper). The addition of a Reinforcing tendon, to be described in the next section, increases the admissable twist angle range to $(\frac{\pi}{6}, \frac{\pi}{2})$.[12–14] In addition, from these papers, by Masic, we conclude the forces in the three bar tensegrity unit are realisable and can be scaled with respect to each other. We now turn our attention to geometry of the structure and writing the equations that describe the reconfiguration of the structure. These equations are vital in deriving the motor command signals that actuate the structure. Choosing the coordinate axes as shown in Fig. 2 we write the coordinates of each node as follows

First Stage		
Nodal Number	Fixed Node?	Coordinates
1	yes	$(r_{base}, 0, 0)$
2	no	$(r\cos\alpha, r\sin\alpha, h)$
3	yes	$(r_{base}\cos(\beta+\alpha), r_{base}\sin(\beta+\alpha), 0)$
4	no	$(r\cos(\beta+2\alpha), r\sin(\beta+2\alpha), h)$
5	yes	$(r_{base}\cos(2\beta+2\alpha), r_{base}\sin(2\beta+2\alpha), 0)$
6	no	$(r\cos(2\beta+3\alpha), r\sin(2\beta+3\alpha), h)$
Second Stage		
7	top platform	$(r_{base}, 0, 2h)$
8	top platform	$(r_{base}\cos(\beta+\alpha), r_{base}\sin(\beta+\alpha), 2h)$
9	top platform	$(r_{base}\cos(2\beta+2\alpha), r_{base}\sin(2\beta+2\alpha), 2h)$

Table 1. Table of nodal coordinates shown in Fig. 2.

where the chosen parameters to describe the geometry of the structure are r, h, and α. From symmetry, the angle β is defined

$$\beta + \alpha = \frac{2\pi}{3}.$$

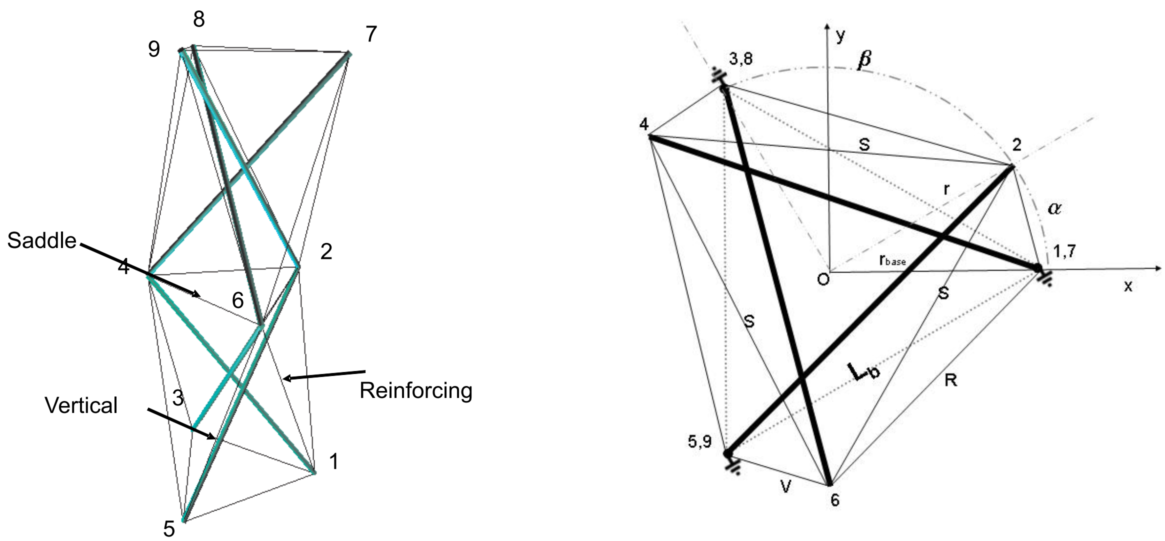

(a) VRML Simulation (b) Top View

Figure 2. Views of 2 stage tensegrity indicating nodal positions and coordinate axes.

The saddle tendon length can be computed by calculating the distance between nodes 4 and 2 as

$$S = \left([r\cos(\frac{2\pi}{3} + \alpha) - r\cos\alpha\ ]^2 + [r\sin(\frac{2\pi}{3} + \alpha) - r\sin\alpha]^2 \right)^{\frac{1}{2}} = r\sqrt{3}. \tag{1}$$

Similarly, the vertical tendon length can be computed by calculating the distance between nodes 2 and 1 as

$$V = \left([r\cos\alpha - r_{base}]^2 + r^2\sin^2\alpha + h^2 \right)^{\frac{1}{2}}, \tag{2}$$

and the reinforcing tendon length can be computed from the distance between nodes 2 and 3 as

$$R = \left([r\cos\alpha - r_{base}\cos(\frac{2\pi}{3})]^2 + [r\sin\alpha - r_{base}\sin(\frac{2\pi}{3})]^2 + h^2 \right)^{\frac{1}{2}}. \tag{3}$$

The parameter r can be shown to depend on h and α, therefore, only two independent parameters are needed to describe the structure completely. Figure 3 can be used to derive the dependence as follows: Apply the law of cosines to $\triangle ABC$

$$(l_{bar}^2 - h^2) = r_{base}^2 + r^2 - 2rr_{base}\cos(\frac{2\pi}{3} + \alpha), \tag{4}$$

and solving for r via the quadratic formula yields

$$r = r_{base}\cos(\frac{2\pi}{3} + \alpha) \pm (r_{base}^2\cos^2(\frac{2\pi}{3} + \alpha) + l_{bar}^2 - h^2 - r_{base}^2)^{\frac{1}{2}}. \tag{5}$$

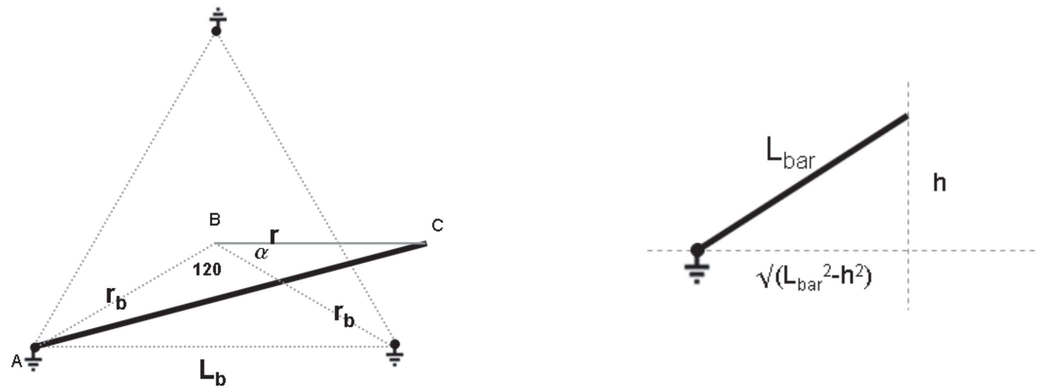

(a) Top View

(b) Side View of a single bar

Figure 3. Geometric relations used to derive the dependence of r on height, h.

Equations (1) and (2) can now be written as functions of h and α, although α will be chosen to be in the admissible range $(\frac{\pi}{6}, \frac{\pi}{2})$ and h will be determined by choice of the function $\dot{h}(t)$. In practice, the bars of the structure will intersect at $\frac{\pi}{3}$ so the admissible range of interest will be either $(\frac{\pi}{6}, \frac{\pi}{3})$ or $(\frac{\pi}{3}, \frac{\pi}{2})$. Since the first term in (5) is always negative for the given range for α, the only positive solution for r will result in taking the positive in the second term.

The addition of the reinforcing tendon is optional and its benefit is to increase stiffness of the structure by locking the infinitesimal mechanism mode that is present in the structure. This feature is highly desirable to increase the stiffness to mass ratio. It should also be noted that the reinforcing tendon allows for a non-unique twist angle, α. That is, a three bar tensegrity unit with only saddle and vertical tendons has only one unique twist angle to be $\alpha = \frac{\pi}{3}$.[15] Since we are considering a symetric deployment, two actuators are needed to deploy the tensegrity: one to control the three saddle tendons and one to control the vertical tendons. This is the minimum configuration of actuators needed to control the structure. The addition of the reinforcing tendon offers two choices. First, to add an additional actuator to control the reinforcing tendons, or second, to find a deployment trajectory that allows for a constant reinforcing tendon length, thus eliminating the need for an extra actuator and benefiting from the added stiffness the tendon offers. The trajectory analysis can be accomplished by examination of (1)-(3).

3. CONSTANT REINFORCING TENDON DEPLOYMENT

As mentioned in the previous section, the addition of the reinforcing tendon is desirable, and to benefit from the tendon without need for its actuation is highly desirable. In order to fully deploy the tower, while maintaining equilibrium, only two actuators are needed. Each actuator controls the lengths of the vertical tendons and the saddle tendons respectively. The lengths of the vertical and saddle tendons must be calculated and controlled over time to maintain a constant reinforcing tendon length, so that the structure will maintain its pre-tensioned equilibrium.

In order to deploy along a trajectory that incorporates a constant reinforcing tendon length, R must be set to a constant value in (3) and then a relation between α and h must be found from this expression. This relation was found numerically and the choice for the constant R was found by the level contours in Fig. 4. The contour at 10 inches was selected since it offers a good range of height variation while maintaining a good distance from the 30 degree twist angle, which results in a slack reinforcing tendon.

In addition, the velocity of the structure height is chosen to be constant, $\dot{h}(t) = k$. Therefore we compute

$$h(t) = \int \dot{h}(t)\, dt = kt + c, \tag{6}$$

and with the boundary conditions $h(0) = h_0$ and $h(t_f) = h_f$, results in

$$h(t) = \frac{h_f - h_0}{t_f} t + h_0, \tag{7}$$

where t_f is the time of deployment.

Given the numerical function $\alpha(h)$ obtained from (3) and (7), the trajectories can be computed by substitution into (1)-(3) resulting in

$$S(t) = r(t)\sqrt{3}, \tag{8}$$

$$V(t) = \left((r(t)^2 + r_{base}^2 - 2r(t)r_{base}\cos(\alpha(h(t))) + h(t)^2\right)^{\frac{1}{2}}, \tag{9}$$

$$R(t) = 10, \tag{10}$$

where

$$r(t) = \left(r_{base}\cos\left(\frac{2\pi}{3} + \alpha(h(t))\right) + \sqrt{(r_{base}^2\cos^2\left(\frac{2\pi}{3} + \alpha(h(t))\right) + l_{bar}^2 - h(t)^2 - r_{base}^2)}\right). \tag{11}$$

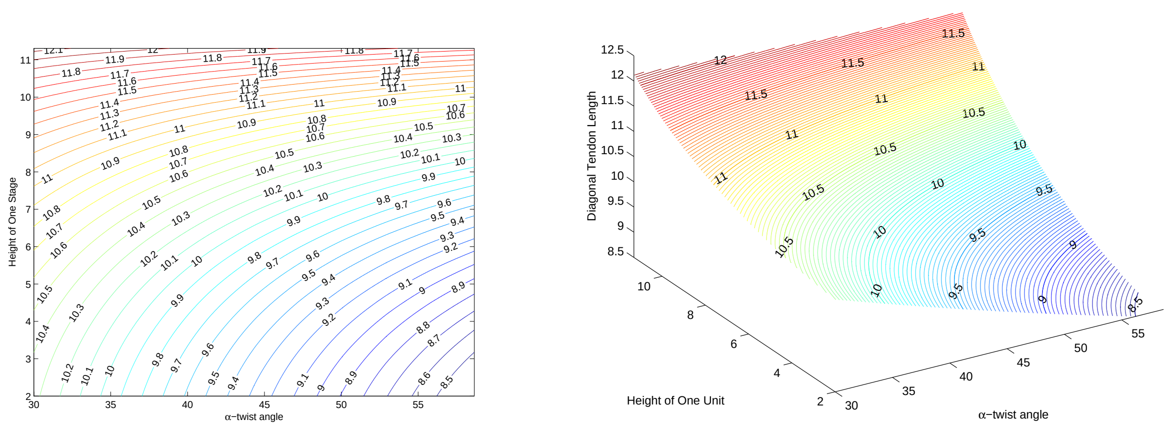

Figure 4. Contour plots of constant Reinforcing tendon length.

4. HARDWARE AND MOTOR CONTROL SYSTEM

The experimental hardware was constructed at the Structural Systems and Control Laboratory at the University of California, San Diego, by Jean-Paul Pinaud and Soren Solari and is shown in Fig. 5. The deployment of the boom was accomplished in 120 seconds and is shown in Fig. 6. The initial height of the structure was 6 inches and the final height is 16.4 inches. The reader should be reminded that the analysis is based on a single stage and multiple stages can be assembled by "stacking" the units on top of each other and reversing the orientation of the bars in each stage. In this paper, we demonstrate two units "stacked" on each other, thus the total height is double the height of one stage. The experiment shown in this paper can be augmented by the addition of another two stages mounted to the top of the structure shown.

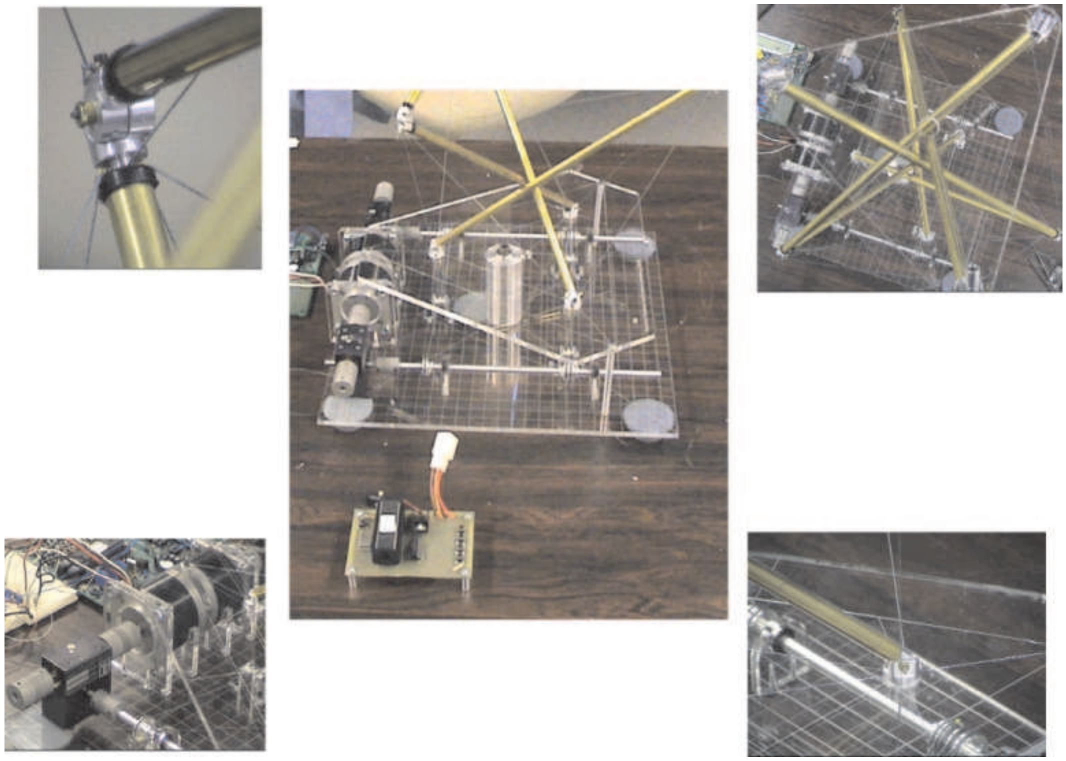

Figure 5. Experimental hardware used to validate the deployment concept. Center - PIC Microcontroller

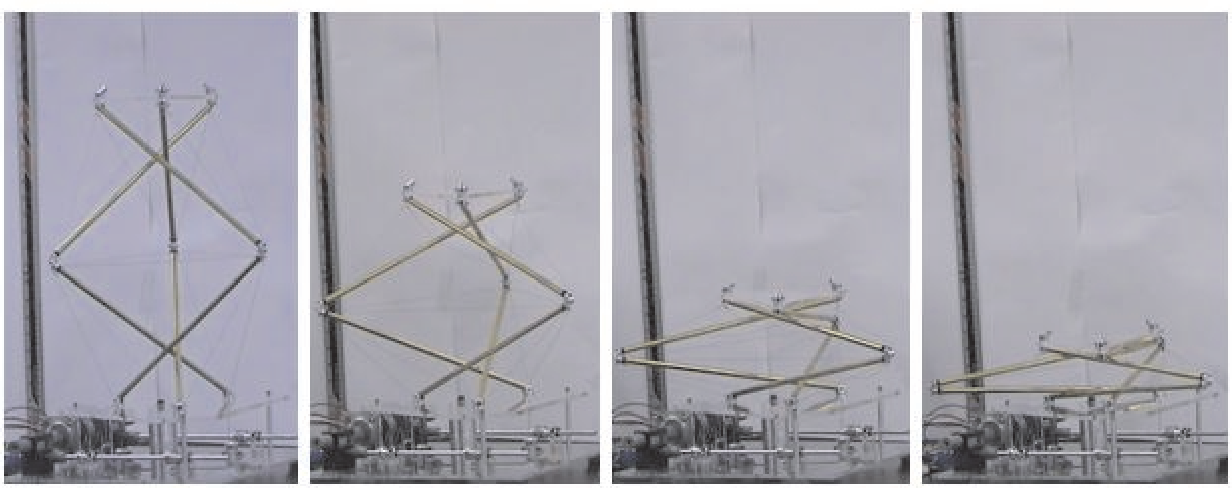

Figure 6. Deployment sequence right to left.

A Programmable Integrated Circuit (PIC) microcontroller and two stepper motors were used to actuate the deployment of the tower. Specifically, the PIC microcontroller was selected because of its portability, minimal cost, and its wide spread use. Stepper motors were the first choice as actuators because of their accuracy and repeatability in open loop position control applications.

The trajectories in (7)-(11) to be programmed into the PIC microcontroller are implemented with the following constants

$$r_{base} = 6 \text{ inches}, \;\; l_{bar} = 12.8 \text{ inches},$$
$$h_0 = 3 \text{ inches}, \;\; h_f = 8.2 \text{ inches},$$
$$t_f = 120 \text{ seconds}.$$

The tendon length vs. time profile is shown in Fig. 7a.

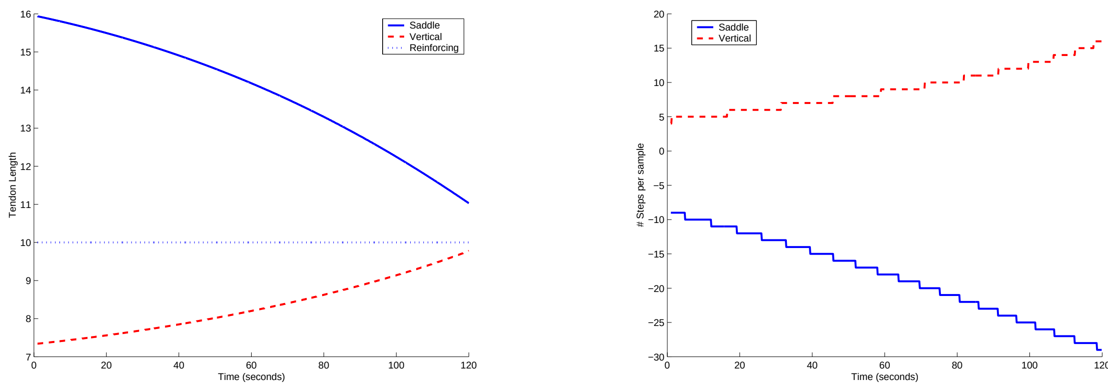

(a) Tendon trajectories for deployment. (b) Stepper motor commands.

Figure 7. Discretization of tendon trajectories to stepper motor control signal.

Because of the limitations on the stepper motor and microcontroller, the tendon length vs. time trajectory for each string cannot be implemented continuously. Instead a total of n samples in time, each sample containing the number of steps the motor should take at a time t, is used as tendon trajectory sent to the motor, as seen in Fig. 7b. The tendon trajectories from Fig. 7a were sampled into $n+1$ samples, where each sample, n_s corresponds to the number of steps the motor must take to change the tendon length from its initial position p_o to the sampled position at a given time p_t. The number of steps per sample s_t is calculated by taking the difference between successive n_s values as

$$s_t = round[n_s(p_t) - n_s(p_{t-1})] \;\; \text{for } t = 1, 2 \ldots n, \tag{12}$$

where $round(*)$ represents rounding to the closest integer. The graph of s_t vs. t is given in Fig. 7b. The discrete nature of the stepper motor forces s_t to be rounded to the nearest integer, since the motor must take an integer number of steps. The number of samples was chosen such that the total number of samples, n summed over all trajectories could fit within the memory of the microcontroller. Constraining $s_t < 256$ steps allows $s_t = 1$ byte of memory. Therefore, the resulting graph is an approximation of the non-linear curves. The approximation is improved as the change in tendon length per step is reduced. The final error in position due to rounding is calculated as

$$n_e = round(n_s(p_n)) - \sum_{t=1}^{n} s_t. \tag{13}$$

Adding n_e, number of steps of error, to the final step trajectory will eliminate the final position error.

5. CONCLUSION

Once the equilibrium conditions are found for a given tensegrity structure's configuration variables, the generation of trajectories can be accomplished using the methodology presented here. In addition, this methodology relies on the use of high stiffness tendon material. The consequences of using a high stiffness tendon allows for the designers to concentrate on the length control of the tendon via position control of the actuating motors, in contrast to implementing force control with length control. The latter, of course, complicates the control strategy significantly.

The use of stepper motors for open loop position control has proven to be an effective method for the deployment and repeatability for this structure. Further research into closed loop control strategies and vibrational control[11] is in progress.

REFERENCES

1. K. Snelson, "Continuous tension, discontinous compression structures," *U.S. Patent 3,169,611* , 1965.
2. C. Sultan, M. Corless, and R. Skelton, "The prestressability problem of tensegrity structures. some analytical solutions.," *to appear in International Jounal of Solids and Structures* , 2001.
3. B. Roth and W. Whiteley, "Tensegrity frameworks," *Transactions of American Mathematical Society* **265**, pp. 419–446, 1981.
4. D. Williamson, R. E. Skelton, and J. Han, "Equilibrium conditions of a tensegrity structures," in *Third World Conference on Structural Control*, (Como, Italy), April 7-12,2002.
5. R. E. Skelton, D. Williamson, and J. Han, "Equilibrium conditions of a class 1 tensegrity structure," in *Advances in the Astronautical Sciences, Spaceflight Mechanics*, **112**(2), p. 927 950, 2002.
6. R. Skelton, J. Helton, R. Adhikari, J. Pinaud, and W. Chan, *An Introduction to the Mechanics of Tensegrity Structures.* CRC Press, Florida, 2001.
7. C. Sultan and R. Skelton, "Tendon control deployment of tensegrity structures," in *Proceedings of SPIE* 5^{th} *Symposium on Smart Structures and Materials 3323*, pp. 455–466, 1998-2.
8. R. Skelton and C. Sultan, "Controllable tensegrity, a new class of smart structures," in *SPIE 4th Annual Symposium on Smart Structures and Materials 3039*, pp. 166–177, (San Diego, CA, USA, March), 1997.
9. S. Pellegrino, "Foldable bar structures," *International Journal of Solids and Structures* **34 (15)**, pp. 1825–1847, 1996.
10. J.-P. Pinaud, M. Masic, and R. E. Skelton, "Path planning for the deployment of tensegrity structures," in *Proceedings of SPIE's 10th Annual International Symposium on Smart Structures and Materials*, (San Diego, CA, USA, March), 2003.
11. W. Chan, F. Bossens, and R. E. Skelton, "Active vibration control of a 3–stage tensegrity structure," in *Proceedings of SPIE's 11th Annual International Symposium on Smart Structures and Materials*, (San Diego, CA, USA, March), 2004.
12. M. Masic and R. Skelton, "Path planing and open-loop shape control of modular tensegrity structures," *AIAA Journal of Guidance, Control, and Dynamics-submitted 12-03-2003* .
13. M. Masic and R. E. Skelton, "Open–loop control of class–2 tensegrity towers," in *Proceedings of SPIE's 11th Annual International Symposium on Smart Structures and Materials*, (San Diego, CA, USA, March), 2004.
14. M. Masic and R. Skelton, "Open-loop shape control of stable unit tensegrity structures," in *Proceedings of 3rd World Congress of Structural Control*, **2**, pp. 439–447, (Como, Italy), 2002.
15. M. Masic, R. Skelton, and P. E. Gill, "Algebraic tensegrity design framework, *to be published*." 2001.